Stem Cell Reports
Resource
ISSCR
OPEN ACCESS

Extraembryonic Endoderm (XEN) Cells Capable of Contributing to Embryonic Chimeras Established from Pig Embryos

Chi-Hun Park,[1,2,*] Young-Hee Jeoung,[1,2] Kyung-Jun Uh,[3] Ki-Eun Park,[1,2,4] Jessica Bridge,[1,2] Anne Powell,[2,4] Jie Li,[5,6,7,8] Laramie Pence,[1,2] Luhui Zhang,[1] Tianbin Liu,[6,7,8] Hai-Xi Sun,[6,7,8] Ying Gu,[6,7,8] Yue Shen,[5,6,7,8,9] Jun Wu,[10,11] Juan-Carlos Izpisua Belmonte,[12] and Bhanu P. Telugu[1,2,4,*]

[1]Animal and Avian Sciences, University of Maryland, College Park, MD 20742, USA
[2]Animal Bioscience and Biotechnology Laboratory, USDA, ARS, Beltsville, MD 20705, USA
[3]Department of Animal and Poultry Sciences, Virginia Polytechnic Institute and State University, Blacksburg, VA 24061, USA
[4]RenOVAte Biosciences Inc, Reisterstown, MD 21136, USA
[5]BGI Education Center, University of Chinese Academy of Sciences, Shenzhen 518083, China
[6]BGI-Shenzhen, Shenzhen, 518083, China
[7]Guangdong Provincial Key Laboratory of Genome Read and Write, Shenzhen, 518120, China
[8]Guangdong Provincial Academician Workstation of BGI Synthetic Genomics, BGI-Shenzhen, Guangdong, China
[9]Shenzhen Engineering Laboratory for Innovative Molecular Diagnostics, Shenzhen, 518120, China
[10]Department of Molecular Biology, University of Texas Southwestern Medical Center, Dallas, TX 75390, USA
[11]Hamon Center for Regenerative Science and Medicine, University of Texas Southwestern Medical Center, Dallas, TX 75390, USA
[12]Salk Institute, La Jolla, San Diego, CA 92037, USA
*Correspondence: chpark@umd.edu (C.-H.P.), btelugu@umd.edu (B.P.T.)
https://doi.org/10.1016/j.stemcr.2020.11.011

SUMMARY

Most of our current knowledge regarding early lineage specification and embryo-derived stem cells comes from studies in rodent models. However, key gaps remain in our understanding of these developmental processes from nonrodent species. Here, we report the detailed characterization of pig extraembryonic endoderm (pXEN) cells, which can be reliably and reproducibly generated from primitive endoderm (PrE) of blastocyst. Highly expandable pXEN cells express canonical PrE markers and transcriptionally resemble rodent XENs. The pXEN cells contribute both to extraembryonic tissues including visceral yolk sac as well as embryonic gut when injected into host blastocysts, and generate live offspring when used as a nuclear donor in somatic cell nuclear transfer (SCNT). The pXEN cell lines provide a novel model for studying lineage segregation, as well as a source for genome editing in livestock.

INTRODUCTION

In the mammalian pre-implantation embryo, separation of trophectoderm (TE) from inner cell mass (ICM) marks the first major cell-fate decision. Soon after, the primitive endoderm (PrE) or hypoblast delaminates from the remainder of late ICM cells, which are now referred to as epiblast (EPI) cells (Cockburn and Rossant, 2010). The bipolar PrE progenitors differentiate into extraembryonic visceral endoderm (VE) and parietal endoderm (PE) of the yolk sac. In most mammals, the yolk sac is widely considered vestigial, except in rodents, where it performs several important functions, such as providing nutritional support, gas exchange, hematopoiesis, and patterning cues to the developing embryo, until the definitive placenta is fully formed. However, the developmental period and functions of yolk sac are not equivalent between species (Bauer et al., 1998; Carter, 2016). Following gastrulation, definitive endoderm (DE) emerges from the primitive streak and replaces PrE from the embryonic region, ultimately giving rise to gut tube and other internal organs. Although DE and PrE are of different lineages, these two cell populations share several molecular and functional properties (Chan et al., 2019; Nowotschin et al., 2019a). Cell lineage–tracing and single-cell transcriptomic studies have found that PrE derivates have become integrated into the gut endoderm, indicating that cell identity between DE and PrE may not be as strict as previously believed (Kwon et al., 2008; Nowotschin et al., 2019b; Viotti et al., 2014).

In culture, three types of stem cells can be established from the mouse embryo: embryonic stem cells (ESCs) from the EPI, trophoblast stem cells from TE, and extraembryonic endoderm (XEN) cells from PrE, which contribute to the embryo proper, the placenta, and the yolk sac, respectively (Rossant, 2008). The XEN cells also can be induced from ESCs by overexpression of PrE-specific genes, *Gata4/6* (Fujikura et al., 2002; Wamaitha et al., 2015), or *Sox17* (McDonald et al., 2014), or by treatment with growth factors (Cho et al., 2012). In rat, XEN cells established from blastocysts have different culture requirements and gene expression profiles compared with mouse XEN cells (Debeb et al., 2009; Galat et al., 2009). While mouse XEN cells mainly contribute to the PE (Lin et al., 2016) in chimeras, rat XEN cells contribute to the VE (Galat et al., 2009). More recently, naive extraembryonic endodermal (nEnd) cells resembling the blastocyst stage PrE-precursors have been developed from mouse and human naive ESCs (Anderson et al., 2017; Linneberg-Agerholm et al., 2019). It is

unclear whether PrE-derived stem cells from nonrodent species have potency similar to mouse or rat (Seguin et al., 2008).

Even though derivation of pESC from EPI cells has proven to be difficult, extraembryonic cells within the early blastocyst outgrowths grow rapidly and outnumber the EPI cells, which can often be misinterpreted as epiblast cells (Keefer et al., 2007; Telugu et al., 2010). Although derivation of extraembryonic endodermal cells in pig embryos currently exist, evidence demonstrating their developmental potential *in vivo* is still lacking (Li et al., 2020; Shen et al., 2019; Talbot et al., 2007). Here we describe detailed characterization of XEN cells from PrE of pig blastocysts. The pXEN cells are stable in culture, undergo self-renewal for extended periods of time, and contribute predominantly to the visceral yolk sac and at a minor level to embryonic gut in chimeras, and can serve as nuclear donors for generating live offspring via somatic cell nuclear transfer (SCNT).

RESULTS

In Vitro Derivation and Expansion of Primary Pig PrE Outgrowths

A central assumption behind the failure to establish pESC is a rapid loss of pluripotency in primary outgrowths (Keefer et al., 2007); however, no details of lineage identities during the derivation phase have been provided. We therefore investigated cellular identity in early blastocyst outgrowths. Zona-free blastocysts seeded onto feeder cells attached and began to spread out within 2 days of culture. After 3 days, larger and flatter TE cells appeared in outgrowths. By 5 days, a distinct PrE layer emerged as a discrete cell layer bordering the ICM (hereafter called "EPI") cells (Figures 1A and S1A), and consisted of two subpopulations that were distinguishable by staining with a structural epithelial marker, KRT18 (Figure 1B): (1) small cells with compact morphology and co-expressing GATA4 and GATA6, and (2) large cells with a loose morphology expressing GATA6 but far less GATA4 (Figure 1C). We noticed that compared with early blastocysts (day 5–6; Figures 1D and 1E), late-stage blastocysts (fully expanded or hatched; day 7–8) exhibited consistent expression of PrE marker genes (Figure S1B) and higher rates of attachment to feeders and emergence of stable PrE outgrowths. Therefore, late-stage blastocysts were used in all subsequent studies.

To monitor lineage segregation in expanding primary ICM outgrowths, we performed a time-course analysis on the expression and localization of NANOG, GATA4, and SOX2. Initially (day 3), cells in the periphery of the early ICM outgrowths were weakly positive for GATA4 and undetectable for NANOG expression (Figures 1F and S1C). By day 5, there was an increase in GATA4+/NANOG + cells. By day 7, >90% of GATA4+ cells coexpressed NANOG (Figure 1G). In contrast, the expression of NANOG was detected in a few, if any EPI cells, while the SOX2+ cells progressively decreased on expansion of colony size with time, indicating a loss of pluripotency (Figures 1G and S1D). Relative quantification of transcripts similarly confirmed high expression of *GATA4*, *GATA6*, and *NANOG*, and low expression of *SOX2* in PrE cells compared with EPI cells (Figure 1H). Besides GATA factors, SALL4, a key stemness marker of XEN cells (Lim et al., 2008), was expressed in the nuclei of small PrE cells but absent in the large PrE. A large fraction (~75%) of SALL4+ cells had nuclear foci of intense histone 3 lysine 27 trimethylation (H3K27me3), a hallmark of the inactive X in female outgrowths (Figures 1I and S1E) (Rugg-Gunn et al., 2010). Consistent with this observation, *XIST* levels were 2-fold higher in SALL4+ PrE cells than in EPI cells (Figure S1F). This reflects the lineage-specific dynamics of H3K27me3 accumulation on the X chromosome, a possible consequence of SALL4 coexpression (Lim et al., 2008).

Cellular Properties and Molecular Signature of pXEN Cells

Self-renewal of XEN cells is dependent on *Sall4* expression (Lim et al., 2008). Stable and consistent appearance of a distinct SALL4+ PrE population in primary outgrowths has prompted us to attempt derivation of pXEN cells. Following 7–9 days of culture, PrE cells developed a distinctive colony boundary, which can be easily dissociated from the EPI cells (Figure S2A) and subcultured to establish primary colonies. Both EPI and PrE colonies displayed epithelial morphology following serial passages (Figure 2A). However, consistent with previous findings, the EPI colonies underwent spontaneous differentiation toward a fibroblast- or neuron-like appearance by passages 5 to 7. The colonies from PrE-derivatives on the other hand, were more stable in culture. The colonies were propagated as flattened colonies and passaged as clumps by mechanical or enzymatic dissociation (Figure 2B), but did not survive passage as single cells even when treated with ROCK inhibitor Y-27632 (Figures 2B and S2B). Following subpassage, the PrE colonies exhibited a characteristic cobblestone monolayer morphology. Cells localized exclusively to the perimeter of the established colonies exhibited strong alkaline phosphatase (ALP) activity and proliferated rapidly as confirmed by PCNA staining (Figure S2C). The density of the feeder cells influenced the colony stability, with the optimal densities ranging from 3 to 4 × 10^4 cells per cm^2. Lower feeder densities (<2 × 10^4 cells/cm^2) resulted in differentiation of cells with associated expression of Vimentin (Figure 2C), and high densities (>1 × 10^5 cells/cm^2) reduced replating efficiency and an

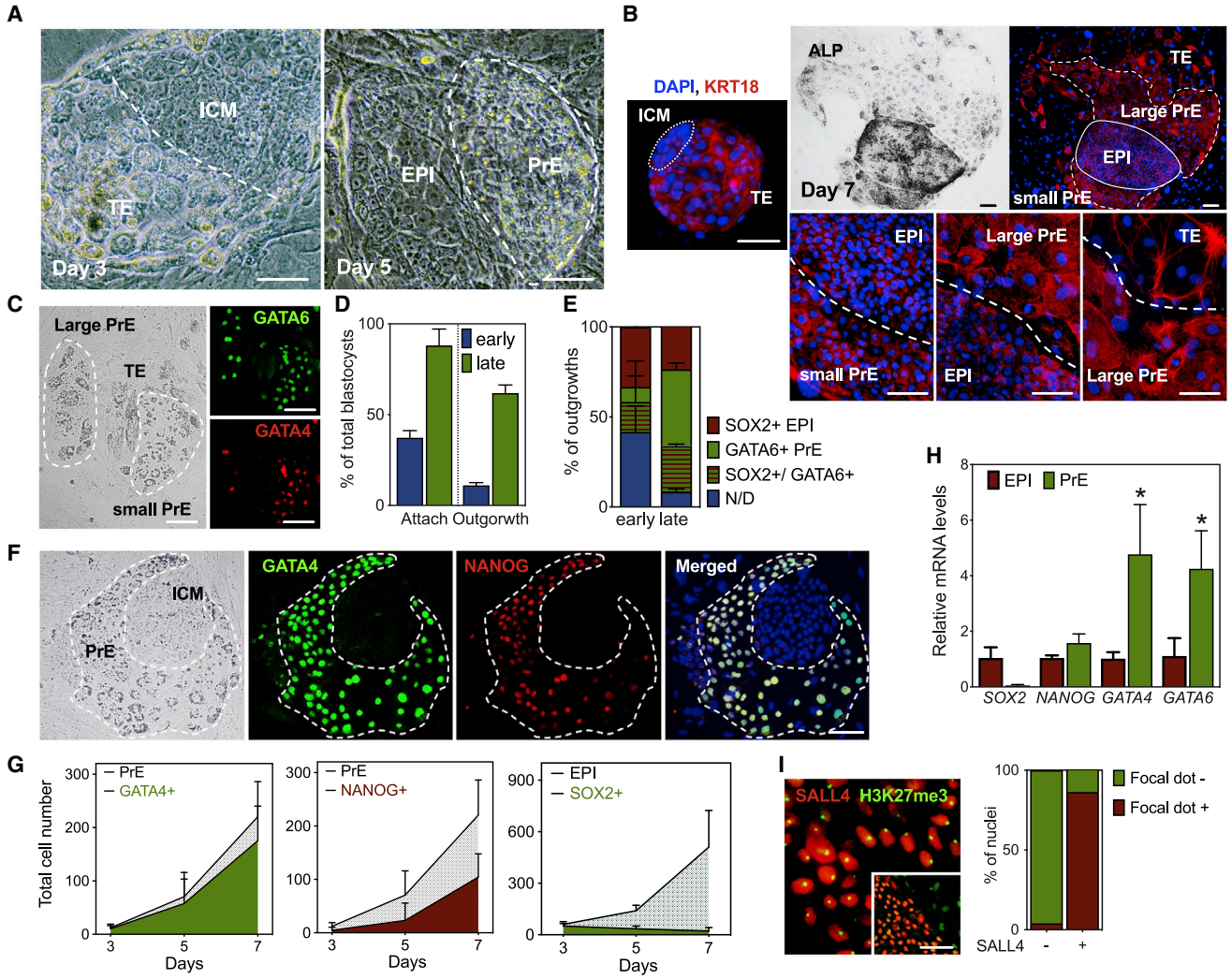

Figure 1. Distinct Subpopulations Arise from the Pig Blastocyst Outgrowths

(A) Phase-contrast image depicting morphologies of blastocyst outgrowths from day 3 and 5 in culture. Subpopulations determined by morphologies were shown with white dotted line (ICM and TE) and circle (PrE).

(B) Representative fluorescence images of KRT18 in the blastocyst (ICM in dotted circle; left) and the primary outgrowth showing mixed populations, including small and large PrE round cells (right). DAPI, nucleus marker.

(C) Phase contrast images and immunostaining of the primary outgrowth 9 days after explanting. In the primary outgrowth, GATA-positive (+) large (solid arrowhead, presumably PE) and small (open arrowhead, nascent PrE) round cells were observed.

(D) The bar graph showing the attachment and outgrowth rates of early and late blastocysts (total blastocysts n = 164). Fourteen independent experiments.

(E) Frequencies of SOX2+ and GATA6+ cells in outgrowths (early n = 9, late n = 10). N/D, not detected.

(F) Immunocytochemical staining exhibiting NANOG and GATA4 expression and its localization within primary outgrowth. PrE part in colony outlined by the dashed line.

(G) Quantitation of the number of NANOG+, GATA4+, SOX2+ nuclei in primary outgrowths cultured on the indicated days after explant (total outgrowths n = 33). Four independent experiments.

(H) Comparison of the transcriptional levels of selected lineage marker genes between PrE cells and EPI cells by qPCR (n = 3 per group).

(I) The expression of H3K27me3 and SALL4 in day 7 primary outgrowth. Scale bar, 100 μm (left). Nuclei were counted (n = 400) and results are shown as percentage of SALL4 positive or negative nuclei with and without H3K27me3 focal dots (right). Scale bars, 50 μm (A) and 100 μm (B, C, F, and I). See also Figure S1 and Table S1.

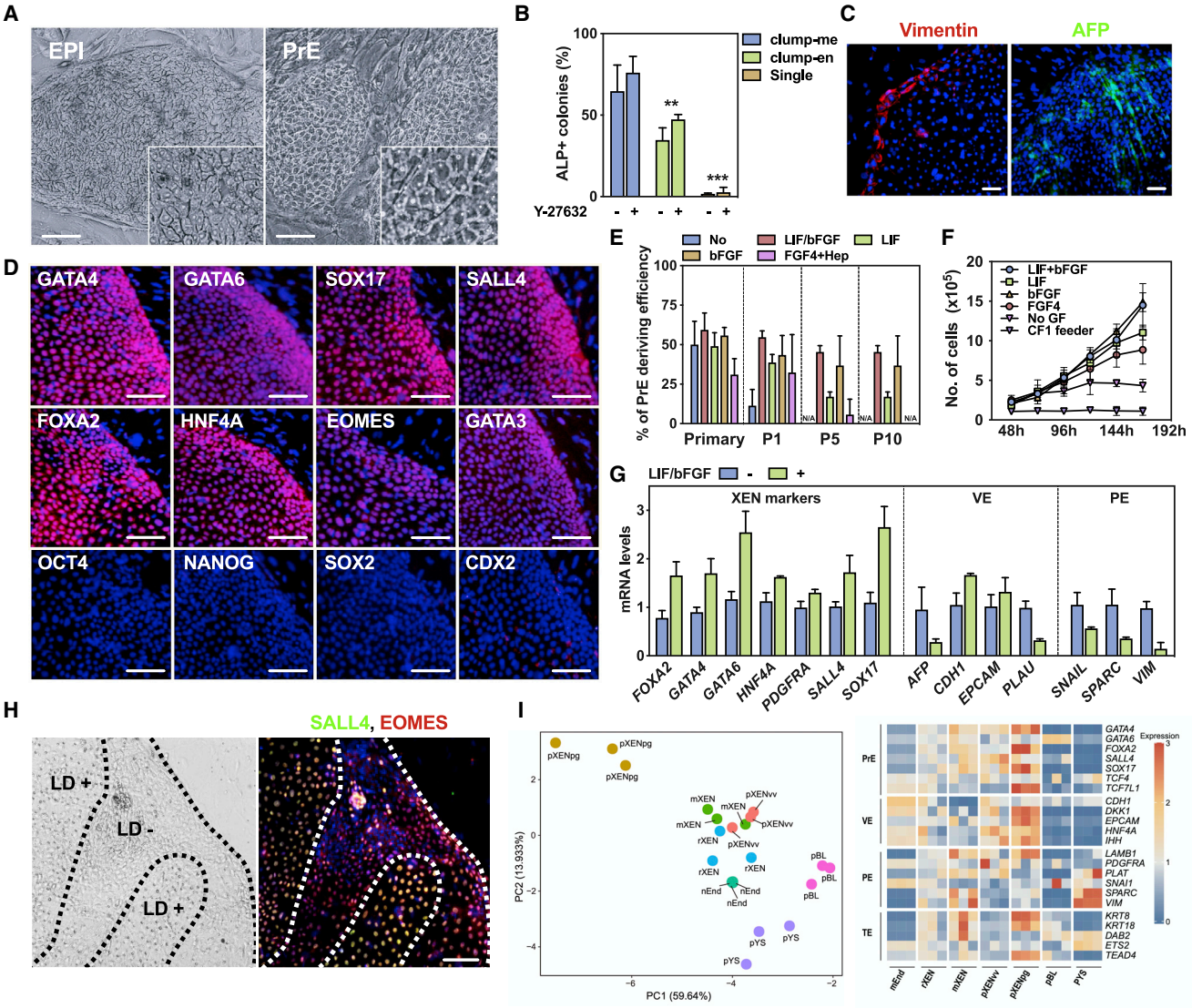

Figure 2. Establishment and Characterization of pXEN Cells

(A) Representative bright-field images of EPI- and PrE-derived cells at passages 3 to 5.

(B) Efficiency of colony formation of pXEN cells passaged as clumps or single cells. The colony-forming activity was greatly impaired when dissociated as single cells. Cells were passaged as clumps by mechanical (clumps-me) or enzymatic dissociation (clumps-en) with Accutase. Colonies n = 20–25 per group.

(C) Representative fluorescence images of PE marker, Vimentin and VE marker, AFP.

(D) Expression of the indicated markers in pXEN at passages 30 to 35.

(E) Effect of growth factors supplementation on PrE derivation. pXEN cells were seeded onto a 6-well plate seeded containing a density of 5×10^4 feeder cells per cm^2 (blastocysts n = 10–12 per group).

(F) Cell number estimated 48 h following passage (n = 3 per group).

(G) qPCR analysis of total RNA isolated from pXEN cells grown in either the presence or absence of LIF/bFGF for 4 days (n = 3 per group).

(H) The expression of SALL4 and EOMES in pXEN cells with or without lipid droplets (LD). Images illustrating presence of LD (+) in the SALL4+ cells. In pXENs, a loss of Sall4 leads to rapid loss of lipid droplet (LD−) outlined by the dashed line.

(I) Transcriptomes of pXEN cells and comparison with analogous derivatives. RNA-seq was performed on two pig XEN cell lines, day 28 pig yolk sac, day 7 pig blastocysts from *in vitro*-fertilized on three biological replicates, as well as published data on related cell lines (mouse and rat XEN cells) were included in the comparison. Principal component analysis (PCA) plot (left) and Heatmap of the levels of selected key XEN-associated genes (right). Scale bars, 100 μm (A, C, D, and H). See also Figure S2 and Table S2.

increase of AFP-positive fibroblastic-like cells below the colonies and dome formation with time (Figures 2C and S2D). Stable pXEN cells expressed PrE-specific markers (GATA4, GATA6, SOX17, SALL4, FOXA2, and HNF4A) and not pluripotent markers (OCT4, SOX2, and NANOG; Figure 2D). Notably, NANOG was no longer detected on passaging. This suggests a possible role for NANOG in PrE specification but not maintenance. While CDX2 is not detectable, other TE-markers EOMES and GATA3 were expressed, consistent with the role of the latter in endodermal specification. Taken together, the molecular signature confirmed the established colonies as XEN cells.

We tested the growth factor requirements of pXEN cells based on observations from mouse (Kunath et al., 2005). Withdrawal of leukemia inhibitory factor (LIF) or basic fibroblast growth factor (bFGF) or both had no impact on primary PrE induction. However, in the omission of both, the cells failed to expand into stable cell lines confirming the growth factor responsiveness (Figure 2E). The colonies that arose in the LIF or FGF4 alone did not proliferate as rapidly as cells cultured with either bFGF, or both LIF and bFGF (Figure 2F). Omission of both growth factors resulted in a reduction in colony formation, with low expression of XEN marker genes *FOXA2*, *GATA4*, *GATA6*, *HNF4A*, *PDGFRA*, *SALL4* and *SOX17,* and high expression of VE- (*AFP* and *PLAU*), and PE-genes (*SNAIL*, *SPARC*, and *VIM*); consistent with spontaneous differentiation (Figure 2G). The pXEN cells could be stably maintained in serum-free N2B27-based defined medium with lower degree of cellular differentiation and expression of VE- and PE-related genes; however, this resulted in a longer cell doubling time (Figures S2E and S2F). One interesting finding is the presence of cellular lipid droplets in the pXEN cells (Figure 2A), which readily disappeared when plated in the absence of growth factors or feeder cells with a concomitant loss of SALL4 expression, but no change in EOMES expression (Figure 2H). The yolk sac endodermal cells are rich in lipids, which serve as a main energy source and abundantly express transcripts involved in lipid metabolism (Cindrova-Davies et al., 2017; Talbot et al., 2007). Visible lipid droplets within the SALL4+ cells are lost within the differentiated derivatives, which could be linked to metabolic switch in differentiating pXEN cells and could be utilized as a non-invasive marker of XEN cell state.

Based on these preliminary trials, we established putative XEN cell lines from *in vivo*-developed (vv, n = 4), *in vitro*-fertilized (vf, n = 13), and parthenogenetically activated (pg, n = 14) pig blastocysts. All lines exhibited stable morphology and marker expression, irrespective of embryonic origin (Figure S2G). However, occasional heterogeneity can be seen in pXENpg lines under different culture conditions (Figure S2G), while essentially retaining growth rates and key marker expression. Uniparental parthenotes have limited developmental potential *in vivo* due to defects in imprinting process among extraembryonic membranes. The heterogeneity noticed in pXENpg derivates may be reflective of similar imprinting defects *in vitro*. The pXEN cells could be maintained with robust proliferative potential in culture for extended passages (>50 passages), and were karyotypically normal (Figure S2H). Global gene expression of pXEN cells was determined by performed RNA sequencing (RNA-seq) analysis on three representative pXENvv lines established from *in vivo* derived embryos and thoroughly characterized by immunostaining in Figure 2D, along with pXENpg lines. Pig blastocysts (d 7) and yolk sac (d 28) and publicly available datasets from rodent XEN cells was used for comparison. Transcriptomic analysis of pXENvv cells confirmed expression of characteristic XEN cell repertoire and clustered closely with mouse XEN cells (Figures 2I and S2I). We further show that pXENs clustered relatively closer to the day 10–11 hypoblast than with day 7–8 pre-implantation or day 28 yolk sac, albeit not closely clustered to any of them (Figure S2J). As expected, uniparental pXENpg lines clustered separately from biparental pXENvv and rodent XEN cells (Figure S2K). The XEN cells readily formed embryoid body (EB)-like structures in suspension culture and underwent differentiation as confirmed by changes in gene expression (Figures S2L and S2M). Importantly, no teratoma development was observed in any recipient mice transplanted with 1×10^6 to 10^7 cells from six representative pXEN cell lines (Table S2) indicating that all injected pXEN cells were committed and not pluripotent cells.

Contribution of pXEN Cells to Chimeras

Mouse XEN cells contribute to PE, whereas rat XEN cells incorporate into both VE and PE lineages in chimeras (Galat et al., 2009; Kunath et al., 2005). Given these disparities, we evaluated the properties of pXEN cells in chimera studies (Figure 3A). To facilitate lineage tracing, we generated a reporter pXEN cell line expressing GFP by knocking-in a constitutive human *UBC* promoter driven GFP encoding sequence downstream of the *COL1A1* locus (hereafter, *pCOL1A* $^{UBC:GFP}$; Figure S3A) using CRISPR/Cas system as previously described (Park et al., 2016). Labeled pXEN (Xnt^{GFP} #3–2) cells were injected as single cells or cell clumps (5–10 cells) into parthenogenetic embryos at the morula (day 4) or early blastocyst stages (day 5). Cells injected as clumps integrated into host embryos more efficiently (77.3%–85.7%) than individual cells (37.5%–47.4%); and cells injected at the blastocyst stage showed better incorporation into ICM (85.7%) than at morula stage (77.3%) (Table S3 and Figure S3B). To evaluate *in vivo* chimeric development, pXEN (Xnt^{GFP} #3–2) cells were similarly injected as clumps into host blastocysts (n = 109). Following overnight culture, the resulting re-expanded

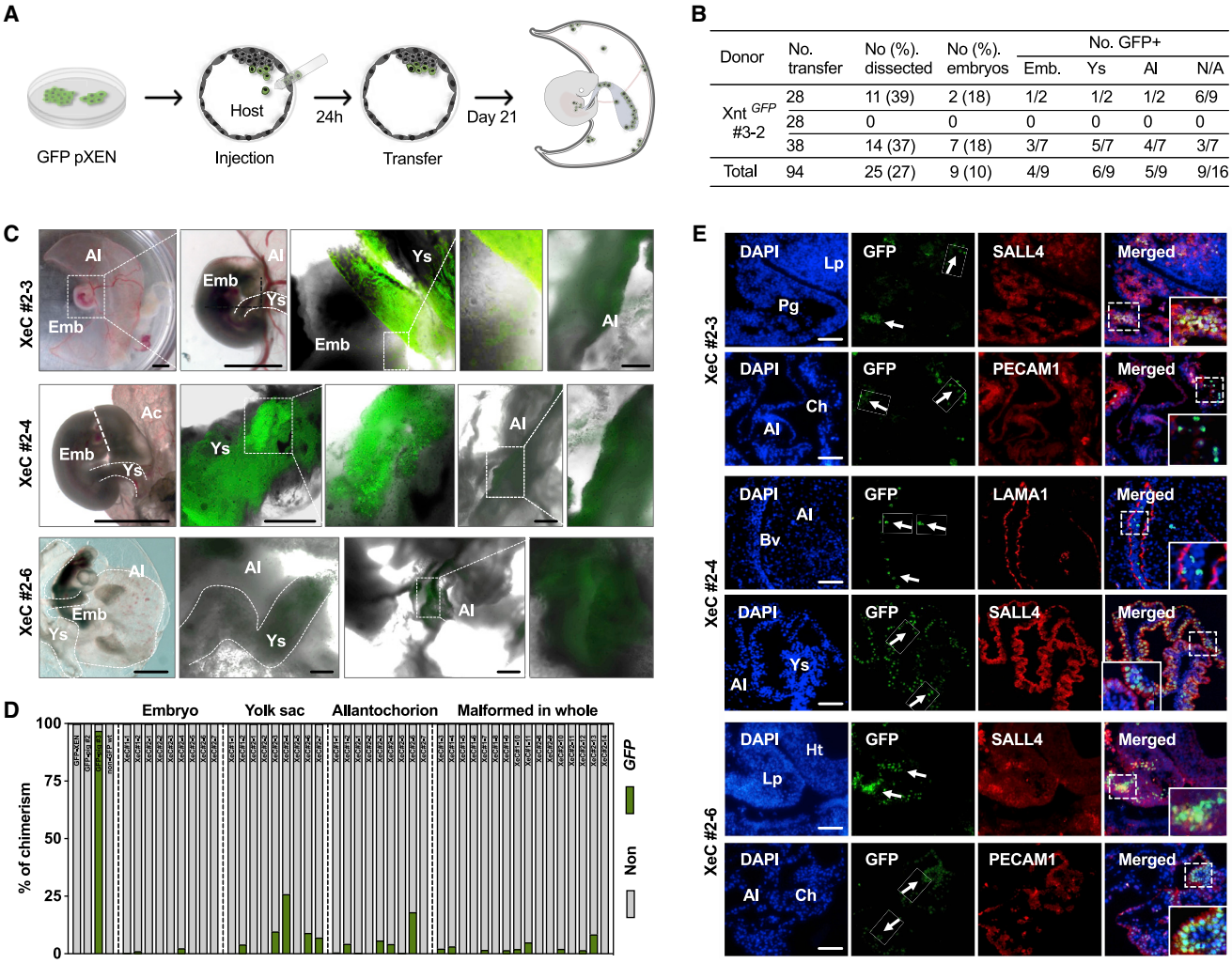

Donor	No. transfer	No (%). dissected	No (%). embryos	No. GFP+ Emb.	Ys	Al	N/A
Xnt ^{GFP} #3-2	28	11 (39)	2 (18)	1/2	1/2	1/2	6/9
	28	0	0	0	0	0	0
	38	14 (37)	7 (18)	3/7	5/7	4/7	3/7
Total	94	25 (27)	9 (10)	4/9	6/9	5/9	9/16

Figure 3. Chimeric Contribution of pXEN Cells to Embryonic and Extraembryonic Lineages in Postimplantation Day 21 Embryos

(A) Schematic representation of the chimera assay.

(B) Table presents a summary of chimera experiments performed by injection of pXEN cells into blastocysts. In the table, Ys, yolk sac; Ac, allantochorion; N/D, not defined (severely retarded fetuses with no fetal or yolk sac parts); and "*" stands for the embryos at the pre-attachment stages (spherical or ovoid).

(C) Representative bright-field and fluorescence merged images of normal (XeC #2–3 and XeC #2–4) and retarded (XeC #2–6) fetuses at day 21 of gestation. Yolk sac outlined by the dashed line, and enlarged view of the region marked by the dashed box is shown in the right. Scale bar, 1 mm (bright field) and 100 μm (fluorescence merged).

(D) Bar graph representing percent contributions of *GFP*-pXEN in chimeras determined by qPCR. Four independent experiments.

(E) Representative sagittal or transverse sections of fetuses showing dual immunofluorescence staining for GFP and SALL4 or LAMA1 or PECAM1 (red) in embryos; the arrows indicate GFP-positive cells derived from injected pXEN cells in sections. Inset are zoom-in magnified images of the dashed box. Nuclei were stained with DAPI (blue). Scale bar, 200 μm. In the figure, Al stands for allantois; Bv, blood vessels; Ch, chorion; Emb, embryo; Hp, heart primordium; Lp, liver primordium; Pg, primitive gut; Ys, yolk sac. See also Figure S3, Table S3, and Table S4.

blastocysts (n = 94) were transferred into three recipient sows (Figure 3B). We decided to observe their chimerism at an early stage of embryonic development because pig yolk sac is vestigial, and undergoes regression at a later time point when the definitive placenta is fully formed. A total of 25 fetuses (27%) were retrieved from two recipients on day 21. Of the recovered fetuses, 4 were normal and 22 were composed of varying degrees of growth impairment with 4 stopped at the preattachment stages of embryo development (spherical or ovoid), 13 showing severe retardation with the embryo lacking portions of fetus and yolk sac, and 5 showing delayed development lacking

extraembryonic vasculature, and displaying head and heart defects. Among the recovered fetuses (n = 9), the injected GFP + cells were found in the yolk sac (6/9) and the fetal membranes (5/9), and a small group of GFP + cells were observed in three fetuses (3/9; Figure 3B). Notably, GPF + cells extensively contributed to the yolk sac in two chimeras (XeC #2–3 and XeC #2–4) with a moderate signal in the allantochorion (Figure 3C). The GFP + cells observed in embryos were from pXEN cells and not due to autofluorescence as confirmed by genomic PCR. Quantification of GFP + cells by qPCR confirmed pXEN cell chimerism at 1.7% in two embryos, and at 12.9% in the yolk sac, and 8% in the allantochorion, signifying active integration and proliferation of pXEN cells during embryogenesis (Figure 3D). As shown in Figure 3E, immunohistochemical analysis with the anti-GFP antibody identified GFP + cells in the embryonic gut of three chimeric fetuses (XeC #2–3, −4, and −6). The GFP + donor cell population integrated predominantly into the visceral endodermal layers, but rarely into the outer mesothelial layers or endothelial cells in the yolk sac (Figure S3C), and to a minor extent populated amnion, allantois, chorion (Figure 3E and Table S4). A few GFP + cells were distributed in the primitive gut (Figure 3E and Figure S3D), providing direct evidence for the contribution of pXEN derivatives to embryonic endoderm of the embryos (Nowotschin and Hadjantonakis, 2020)

Generation of Live Offspring from pXEN Cells via SCNT

To test the utility of pXEN cells as nuclear donors, we performed SCNT with two pXEN cell lines and three fetal fibroblasts (FF). No significant differences in the cleavage (71.9%–88.0%) and blastocyst formation rates (32.0%–43.8%) were observed between the cell types (Table S5). Next, we compared the cloning efficiency by using GFP-labeled pXEN cell line used in the chimera assay (above), alongside previously published crossbred knockout FF $^{NGN3-/-}$ as controls (Sheets et al., 2018). A total of 222 cloned embryos reconstituted from pXEN (Xnt^{GFP} #3–2, n = 61) and FF $^{NGN3-/-}$ (n = 161) were collectively transferred into two surrogate gilts to exclude confounding variables associated with recipient animals affecting the outcome. Following embryo transfers, one pregnancy was established, and eight cloned piglets delivered at term. Three of the eight piglets were GFP positive and black coated (4.9%) confirming the *GFP* Ossabaw pXEN cell origin, while five piglets were white coated and GFP negative and therefore from the FF $^{NGN3-/-}$ (3.1%; Figure 4A). As expected, the piglets exhibited ubiquitous expression of GFP in all tissues (Figure 4B). The genotype of the offspring was confirmed by PCR (Figure 4C).

In an additional experiment, we wanted to compare the potency of *GFP*-pXEN cells with the original donor somatic cells (FF^{GFP} #3) used for deriving reporter pXEN cell line (Xnt^{GFP} #3–2). Despite being genetically identical, all recipients from founder FFs failed to establish a pregnancy or lost during early pregnancy, while other donor cells (*pCOL1A*^{Attp}) that derived from the same fetus had high developmental competence and cloning efficiency (8.2%). One potential explanation is the epigenetic disruptions within cells caused by transfection that may have compromised embryonic development, which is likely reset during cloned XEN cell derivation (Kuroiwa et al., 2004). It remains to be seen if this could be applicable to other cells that failed to generate live offspring by SCNT. Although our investigations so far have only been on a small scale, our findings do nevertheless suggest that the pXEN cells are able to support full-term development following SCNT.

DISCUSSION

Over the past 3 decades, multiple studies have reported that under conventional ESC derivation conditions and without major chemical or genetic interventions (Bogliotti et al., 2018; Gao et al., 2019), the EPI fraction of primary blastocyst outgrowths from pigs and other livestock fail to proliferate and are rapidly overtaken by rapidly expanding extraembryonic cells (Keefer et al., 2007). The main goal of this study was to take a systematic and in-depth look at the derivation, establishment, and characterization of pXEN cells. Our findings identified that induction of PrE lineage is marked by NANOG and GATA4 coexpression. Mutual antagonism between NANOG and GATA4/6 has been implicated in early cell-fate decisions between EPI and PrE (Chazaud et al., 2006; Mitsui et al., 2003; Plusa et al., 2008), and the cell sorting model for EPI/PrE formation is generally considered to be conserved across many mammalian species. However, contrary to previous findings, recent evidence suggests that Nanog expression is required not only for the formation of EPI but also for proper PrE formation (Messerschmidt and Kemler, 2010). Interestingly, several lines of evidence can be found confirming the expression of NANOG in the hypoblast of pig prestreak stage (day 9–11) embryos; however, its precise role has not been defined yet (Kobayashi et al., 2017; Ramos-Ibeas et al., 2019; Wolf et al., 2011). Coexpression of NANOG/GATA4 in emerging PrE population in pigs marks a key difference in early lineage specification from mouse. That said, established pXEN cells share close similarities to mouse and rat XEN cells in their culture characteristics, and the molecular signatures (including high expression of *FOXA2*, *GATA4*, *GATA6*, *HNF4A*, *PDGFRA*, *SALL4* and *SOX17*), with a key exception being a failure to establish pXEN cells in FGF4-based medium, and intolerance to dispersal as single cells.

Generation of embryonic chimeras has been considered the most stringent test of stem cell differentiation potential

A

Donor	Cell type	No. transferred	Pregnancy	Term	#Efficiency (%)
FF ^{Attp}	Fibroblasts	134	1/1	11	8.2
FF ^{GFP}	Fibroblasts	291	0/3	-	0
Xnt ^{GFP}	pXEN	61		3	4.9
NGN3$^{-/-}$	Fibroblasts	161	1/2	5	3.1
Total		222		8	3.6

B

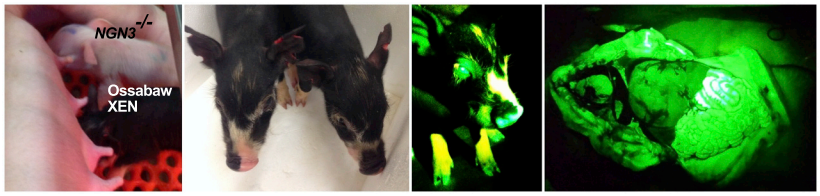

C

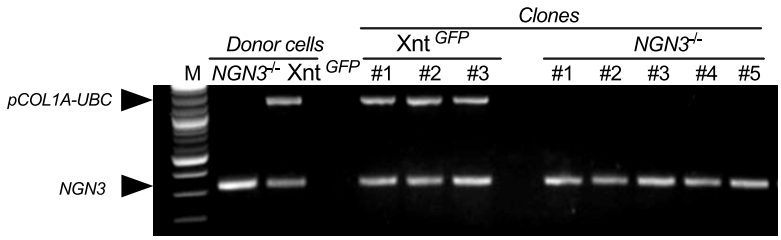

Figure 4. Generation of Viable Cloned Piglets Using pXEN or Fibroblasts

(A) Summary of SCNT experiments. #Cloning efficiency was obtained by calculating total no. fetuses or piglets/total no. embryos transferred. $data obtained from our previous study. *$NGN3^{-/-}$ cells originated from our previous report (Sheets et al., 2018). All the FFs and pXEN cells except for $NGN3^{-/-}$ cells used as SCNT donors were derived from the same fetus (female Ossabow fetal fibroblast #6).

(B) Representative images showing 10-day-old $NGN3^{-/-}$ white (outbred)- and pXEN Black (Ossabaw)-coated littermates. The fluorescence images of live GFP + piglets and whole organs taken with blue light illumination showing ubiquitous expression of *GFP* transgene, and confirming the pXEN cell as nuclear donors.

(C) A representative gel image of the 1.2-kb amplicon with primers within and outside of the targeting vector confirming site-specific knockin was generated. See also Table S5.

in vivo (Mascetti and Pedersen, 2016). This study demonstrates that pXEN cells possess PrE-like properties and a less committed endodermal naive state as confirmed by a marked integration to visceral yolk sac, as well as parts of placenta in chimeras. Freshly isolated ICMs are capable of widespread contribution, including germline colonization in pig chimeras (Nagashima et al., 2004). Despite this, the pluripotent EPI or iPS cells were preferentially engrafted into extraembryonic tissues (Ezashi et al., 2011; Fujishiro et al., 2013; West et al., 2010). It is likely that in the absence of defined conditions, the stem cell cultures are unstable and reside in an XEN-like state and integrate into extraembryonic lineages (Zhao et al., 2015). This study also identified that pXEN cells possess naive endodermal PrE-like properties, as evidenced by marked integration into the DE. Of interest, and consistent with the observations from mouse studies where VE participated in the formation of the primitive gut tube (Chan et al., 2019; Kwon et al., 2008; Nowotschin et al., 2019b), pXEN cells are not exclusively confined to extraembryonic regions but go on to embryonic endodermal tissues *in vivo* that could be conserved among mammals (Nowotschin et al., 2019a). This finding is of potential interest for interspecies chimera efforts for generating humanized organs (e.g., liver, pancreas) in pigs via blastocyst complementation (Kobayashi et al., 2010; Matsunari et al., 2013; Wu et al., 2017). Evidence from the present study demonstrates engraftment potential of pXEN cells to be restricted to endodermal lineage in the host embryo. In this regard, human XEN or nEnd cells could be an ideal source for interspecies chimerism efforts to preclude donor contribution to undesirable organs (e.g., germ cell or neural lineage), a likely outcome with the use of ESC/iPS cells (Masaki et al., 2016; Rashid et al., 2014). Although the present study convincingly supports the lineage potency of pXEN *in vivo*, long-term cell survival and function in host environment would need to be investigated and will be an integral part of future research for use in regenerative medicine approaches.

To date, while cloned animals have been generated using various somatic cell types, SCNT remains an inefficient process with various success rate of 1% to 10% and their efficiencies are greatly influenced by multiple factors including the donor cell types (Keefer, 2015; Kurome et al., 2013; Long et al., 2014). However, the ability of the nuclei of cells from extraembryonic lineages to serve as nuclear donors has not been evaluated. As evidenced from this study, the XEN cells can support full-term development via SCNT. We also noted that a transfected cell, which was genetically identical to the pXEN cell donor, failed to generate live offspring despite repeated attempts. Such

overt developmental defects are frequently seen in embryos cloned by nuclei from transfected cells. Indeed, the adverse effect of transfection has been a main concern for genetic modification of donor cells for producing transgenic animals (Kurome et al., 2013). The precise molecular basis of how the developmental competence has been regained following the derivation of pXEN cell lines requires further investigation.

In summary, the recent report on expanded potential stem cells (Gao et al., 2019), combined with the observation of XEN-like cells representing an intermediate state to pluripotency during chemical-induced reprogramming (Zhao et al., 2015), provide a basis for comparative studies of lineage-specific stem cells. This study on pXEN cells will serve to improve our understanding of the basic developmental process leading to mechanisms of early cell-fate decision and pluripotency.

EXPERIMENTAL PROCEDURES

More detailed description of Materials and Methods is provided in the Supplementary Information. Brief description of Materials and Methods is outlined as follows.

Animal Experimental Assurance

All experiments involving live animals were performed in accordance with the approved guidelines of the Beltsville Agricultural Research Service and Thomas D. Morris Inc., Institutional Animal Care and Use Committee (IACUC). All experimental protocols involving live animals were approved by the IACUC committee.

Establishment and Maintenance of Pig XEN Cells

Embryonic explants and pXEN cells were cultured on a feeder layer of early passage (>4) CF-1 mouse embryonic fibroblasts (MEF) cells mitotically inactivated by treatment with mitomycin-C (3 h, 10 μg/mL) at a density of 3 to 5 × 10^5 cells per cm^2. At least 2 h before the start of the experiment, the MEF medium was aspirated and replaced with "standard ES medium," which included DMEM/Nutrient Mixture Ham's F12 (DMEM/F-12; Gibco) supplemented with 15% ES-qualified fetal calf serum (HyClone), 1 mM sodium pyruvate, 2 mM L-glutamine, 100 units/mL penicillin-streptomycin, 0.1 mM 2-β-mercaptoethanol, 1% nonessential amino acids (Gibco), with various combination of growth factors; 10 ng/mL human recombinant LIF (hrLIF; Milipore) and 10 ng/mL human recombinant basic fibroblast growth factor (hrbFGF; R&D Systems). Following initial plating, attachment and outgrowth development, the medium was refreshed on day 3, followed by media exchange every 2 days. After 7 to 8 days of culture, the primary outgrowths were mechanically dissociated into small clumps, and transferred onto fresh feeders for passaging.

Embryo Production, Manipulation, and Transfer

The *in vivo* and *in vitro* embryo production were performed as described previously (Park et al., 2016; Sheets et al., 2018). The surrogate recipients were synchronized by oral administration of progesterone analog Regumate (Merck) for 14 to 16 days. Animals in natural estrus on the day of surgery were used as recipients for SCNT embryo transfers (into oviduct), and at days 5 to 6 after natural heat were used for blastocyst transfer (into uterus) for generating chimeras. Surgical procedure was performed under a 5% isoflurane general anesthesia following induction with TKX (Telazol 100 mg/kg, ketamine 50 mg/kg, and xylazine 50 mg/kg body weight) administered intramuscularly. Pregnancies were confirmed by ultrasound on day 27 following transfer. Cloned piglets were delivered at day 117 of pregnancy by natural parturition.

RNA and DNA Preparation and qPCR

For isolation of genomic DNA (gDNA) from cells and tissues, the QIAamp mini DNA Kit (Qiagen) was used according to the manufacturer's instructions. Total RNA was isolated using Trizol plus RNeasy mini kit (Qiagen) and mRNA from individual blastocysts was extracted using the Dynabeads mRNA Direct Kit (Dynal Asa). Synthesis of cDNA was performed using a High Capacity cDNA Reverse transcription kit (Applied Biosystems according to the manufacturer's instructions). The QIAseq FX Single-Cell RNA Library kit (Qiagen) was used for Illumina library preparation and transcriptomics analysis. Relative quantification of mRNA levels was carried out using SYBR Green technology on an ABI 7500 Fast Real-Time PCR system (Applied Biosystems).

Generating of a GFP-KI Reporter

To establish green fluorescent protein (*GFP*) gene-based reporter pXEN cell line, we established a site-specific knockin (KI) Ossabaw FFs. Briefly, a precomplexed Cas9 protein and sgRNA ribonucleoprotein (RNP) complex was nucleofected (Amaxa) alongside a ubiquitous promoter (*UBC*) driven *GFP* (Sanger Institute) vector to target downstream of a ubiquitously expressed *COL1A1* locus to ensure stable expression of transgenes. After a day of transfection, the GFP-positive (GFP+) cells were sorted by flow cytometry (Becton Dickinson) and GFP + single cells were replated into wells of a 96-well plate for expansion. After 10 to 15 days, an aliquot of cells was lysed and were directly used as a template for PCR with screening primers. Using GFP-labeled pXEN cells, live animals were generated by SCNT.

Chimera Assay

A candidate $pCOL1A^{UBC:GFP}$ pXEN cell line (Xnt^{GFP} #3–2) with stable expression of GFP and XEN markers was used for chimera testing. The cells were pretreated with Rho Kinase (ROCK) inhibitor Y-27632 (10 μM; StemCell Technologies) for 2 h and dissociated with Accutase at 38.5°C for 5 min followed by gentle pipetting. Approximately three to four small clumps (10–15 cells) were injected per blastocyst (Figure S3B). After 20 to 24 h of culture, injected blastocysts (n = 94) were surgically transferred into the upper part of each uterine horn through needle puncture in recipients at days 5 to 6 of the estrous cycle (D0 = onset of estrus; n = 3).

Data and Code Availability

A total of 12 RNA-seq datasets used in this study have been deposited in the CNSA (https://db.cngb.org/cnsa/) of CNGBdb with accession code CNP0000388, and NCBI Gene Expression Omnibus

(http://www.ncbi.nlm.nih.gov/geo) under accession number GSE128149.

SUPPLEMENTAL INFORMATION

Supplemental Information can be found online at https://doi.org/10.1016/j.stemcr.2020.11.011.

AUTHOR CONTRIBUTIONS

C.P. and B.T. conceived the project and designed the experiments; C.P., Y.J., K.U., and J.B. established and performed characterization of embryonic outgrowths and pXEN cells; K.P. and A.P. performed the knockin and generated the *GFP* reporter lines used for generating GFP pXEN cells used in chimera experiments; C.P., J.L., L.P., L.Z., T.L., J.S., Y.G., Y.S., and J.W. generated the libraries and transcriptomic analysis; C.P. and B.T. wrote the initial draft; C.P., J.W., J.C.B., and B.T. revised the manuscript based on the input from all authors. All authors approved final draft for submission.

CONFLICTS OF INTEREST

K.P., A.P., and B.T. serve as consultants at RenOVAte Biosciences Inc. (RBI). B.T. and K.P. are the founding members of RBI. All remaining authors declare no competing or conflicts of interest.

ACKNOWLEDGMENTS

This research was supported by AFRI Grants# 2015-67015-22845 and 2018-67015-27575 from the USDA National Institute of Food and Agriculture, and 1 R01 HD092304-01A1 from NICHD, NIH to B.T.; Guangdong Provincial Key Laboratory of Genome Read and Write (No. 2017B030301011), Guangdong Provincial Academician Workstation of BGI Synthetic Genomics (No. 2017B090904014), Shenzhen Engineering Laboratory for Innovative Molecular Diagnostics (DRC-SZ[2016]884) and Shenzhen Peacock Plan (No.. KQTD20150330171505310)

Received: July 13, 2020
Revised: November 16, 2020
Accepted: November 17, 2020
Published: December 17, 2020

REFERENCES

Anderson, K.G.V., Hamilton, W.B., Roske, F.V., Azad, A., Knudsen, T.E., Canham, M.A., Forrester, L.M., and Brickman, J.M. (2017). Insulin fine-tunes self-renewal pathways governing naive pluripotency and extra-embryonic endoderm. Nat. Cell Biol. *19*, 1164–1177.

Bauer, M.K., Harding, J.E., Bassett, N.S., Breier, B.H., Oliver, M.H., Gallaher, B.H., Evans, P.C., Woodall, S.M., and Gluckman, P.D. (1998). Fetal growth and placental function. Mol. Cell. Endocrinol. *140*, 115–120.

Bogliotti, Y.S., Wu, J., Vilarino, M., Okamura, D., Soto, D.A., Zhong, C., Sakurai, M., Sampaio, R.V., Suzuki, K., Izpisua Belmonte, J.C., et al. (2018). Efficient derivation of stable primed pluripotent embryonic stem cells from bovine blastocysts. Proc. Natl. Acad. Sci. U. S. A. *115*, 2090–2095.

Carter, A.M. (2016). IFPA senior award lecture: mammalian fetal membranes. Placenta *48*, S21–S30.

Chan, M.M., Smith, Z.D., Grosswendt, S., Kretzmer, H., Norman, T.M., Adamson, B., Jost, M., Quinn, J.J., Yang, D., Jones, M.G., et al. (2019). Molecular recording of mammalian embryogenesis. Nature *570*, 77–82.

Chazaud, C., Yamanaka, Y., Pawson, T., and Rossant, J. (2006). Early lineage segregation between epiblast and primitive endoderm in mouse blastocysts through the Grb2-MAPK pathway. Dev. Cell *10*, 615–624.

Cho, L.T., Wamaitha, S.E., Tsai, I.J., Artus, J., Sherwood, R.I., Pedersen, R.A., Hadjantonakis, A.K., and Niakan, K.K. (2012). Conversion from mouse embryonic to extra-embryonic endoderm stem cells reveals distinct differentiation capacities of pluripotent stem cell states. Development *139*, 2866–2877.

Cindrova-Davies, T., Jauniaux, E., Elliot, M.G., Gong, S., Burton, G.J., and Charnock-Jones, D.S. (2017). RNA-seq reveals conservation of function among the yolk sacs of human, mouse, and chicken. Proc. Natl. Acad. Sci. U. S. A. *114*, E4753–E4761.

Cockburn, K., and Rossant, J. (2010). Making the blastocyst: lessons from the mouse. J. Clin. Invest *120*, 995–1003.

Debeb, B.G., Galat, V., Epple-Farmer, J., Iannaccone, S., Woodward, W.A., Bader, M., Iannaccone, P., and Binas, B. (2009). Isolation of Oct4-expressing extraembryonic endoderm precursor cell lines. PLoS One *4*, e7216.

Ezashi, T., Matsuyama, H., Telugu, B.P., and Roberts, R.M. (2011). Generation of colonies of induced trophoblast cells during standard reprogramming of porcine fibroblasts to induced pluripotent stem cells. Biol. Reprod. *85*, 779–787.

Fujikura, J., Yamato, E., Yonemura, S., Hosoda, K., Masui, S., Nakao, K., Miyazaki Ji, J., and Niwa, H. (2002). Differentiation of embryonic stem cells is induced by GATA factors. Genes Dev. *16*, 784–789.

Fujishiro, S.H., Nakano, K., Mizukami, Y., Azami, T., Arai, Y., Matsunari, H., Ishino, R., Nishimura, T., Watanabe, M., Abe, T., et al. (2013). Generation of naive-like porcine-induced pluripotent stem cells capable of contributing to embryonic and fetal development. Stem Cells Dev. *22*, 473–482.

Galat, V., Binas, B., Iannaccone, S., Postovit, L.M., Debeb, B.G., and Iannaccone, P. (2009). Developmental potential of rat extraembryonic stem cells. Stem Cells Dev. *18*, 1309–1318.

Gao, X., Nowak-Imialek, M., Chen, X., Chen, D., Herrmann, D., Ruan, D., Chen, A.C.H., Eckersley-Maslin, M.A., Ahmad, S., Lee, Y.L., et al. (2019). Establishment of porcine and human expanded potential stem cells. Nat. Cell Biol. *21*, 687–699.

Keefer, C.L. (2015). Artificial cloning of domestic animals. Proc. Natl. Acad. Sci. U. S. A. *112*, 8874–8878.

Keefer, C.L., Pant, D., Blomberg, L., and Talbot, N.C. (2007). Challenges and prospects for the establishment of embryonic stem cell lines of domesticated ungulates. Anim. Reprod. Sci. *98*, 147–168.

Kobayashi, T., Yamaguchi, T., Hamanaka, S., Kato-Itoh, M., Yamazaki, Y., Ibata, M., Sato, H., Lee, Y.S., Usui, J., Knisely, A.S., et al. (2010). Generation of rat pancreas in mouse by interspecific blastocyst injection of pluripotent stem cells. Cell *142*, 787–799.

Kobayashi, T., Zhang, H., Tang, W.W.C., Irie, N., Withey, S., Klisch, D., Sybirna, A., Dietmann, S., Contreras, D.A., Webb, R., et al. (2017). Principles of early human development and germ cell program from conserved model systems. Nature *546*, 416–420.

Kunath, T., Arnaud, D., Uy, G.D., Okamoto, I., Chureau, C., Yamanaka, Y., Heard, E., Gardner, R.L., Avner, P., and Rossant, J. (2005). Imprinted X-inactivation in extra-embryonic endoderm cell lines from mouse blastocysts. Development *132*, 1649–1661.

Kuroiwa, Y., Kasinathan, P., Matsushita, H., Sathiyaselan, J., Sullivan, E.J., Kakitani, M., Tomizuka, K., Ishida, I., and Robl, J.M. (2004). Sequential targeting of the genes encoding immunoglobulin-mu and prion protein in cattle. Nat. Genet. *36*, 775–780.

Kurome, M., Geistlinger, L., Kessler, B., Zakhartchenko, V., Klymiuk, N., Wuensch, A., Richter, A., Baehr, A., Kraehe, K., Burkhardt, K., et al. (2013). Factors influencing the efficiency of generating genetically engineered pigs by nuclear transfer: multifactorial analysis of a large data set. BMC Biotechnol. *13*, 43.

Kwon, G.S., Viotti, M., and Hadjantonakis, A.K. (2008). The endoderm of the mouse embryo arises by dynamic widespread intercalation of embryonic and extraembryonic lineages. Dev. Cell *15*, 509–520.

Li, Y., Wu, S., Yu, Y., Zhang, H., Wei, R., Lv, J., Cai, M., Yang, X., Zhang, Y., and Liu, Z. (2020). Derivation of porcine extraembryonic endoderm-like cells from blastocysts. Cell Prolif *53*, e12782.

Lim, C.Y., Tam, W.L., Zhang, J., Ang, H.S., Jia, H., Lipovich, L., Ng, H.H., Wei, C.L., Sung, W.K., Robson, P., et al. (2008). Sall4 regulates distinct transcription circuitries in different blastocyst-derived stem cell lineages. Cell Stem Cell *3*, 543–554.

Lin, J., Khan, M., Zapiec, B., and Mombaerts, P. (2016). Efficient derivation of extraembryonic endoderm stem cell lines from mouse postimplantation embryos. Sci. Rep. *6*, 39457.

Linneberg-Agerholm, M., Wong, Y.F., Romero Herrera, J.A., Monteiro, R.S., Anderson, K.G.V., and Brickman, J.M. (2019). Naive human pluripotent stem cells respond to Wnt, Nodal and LIF signalling to produce expandable naive extra-embryonic endoderm. Development *146*, dev180620.

Long, C.R., Westhusin, M.E., and Golding, M.C. (2014). Reshaping the transcriptional frontier: epigenetics and somatic cell nuclear transfer. Mol. Reprod. Dev. *81*, 183–193.

Masaki, H., Kato-Itoh, M., Takahashi, Y., Umino, A., Sato, H., Ito, K., Yanagida, A., Nishimura, T., Yamaguchi, T., Hirabayashi, M., et al. (2016). Inhibition of apoptosis overcomes stage-related compatibility barriers to chimera formation in mouse embryos. Cell Stem Cell *19*, 587–592.

Mascetti, V.L., and Pedersen, R.A. (2016). Contributions of mammalian chimeras to pluripotent stem cell research. Cell Stem Cell *19*, 163–175.

Matsunari, H., Nagashima, H., Watanabe, M., Umeyama, K., Nakano, K., Nagaya, M., Kobayashi, T., Yamaguchi, T., Sumazaki, R., Herzenberg, L.A., et al. (2013). Blastocyst complementation generates exogenic pancreas in vivo in apancreatic cloned pigs. Proc. Natl. Acad. Sci. U. S. A. *110*, 4557–4562.

McDonald, A.C., Biechele, S., Rossant, J., and Stanford, W.L. (2014). Sox17-mediated XEN cell conversion identifies dynamic networks controlling cell-fate decisions in embryo-derived stem cells. Cell Rep. *9*, 780–793.

Messerschmidt, D.M., and Kemler, R. (2010). Nanog is required for primitive endoderm formation through a non-cell autonomous mechanism. Dev. Biol. *344*, 129–137.

Mitsui, K., Tokuzawa, Y., Itoh, H., Segawa, K., Murakami, M., Takahashi, K., Maruyama, M., Maeda, M., and Yamanaka, S. (2003). The homeoprotein Nanog is required for maintenance of pluripotency in mouse epiblast and ES cells. Cell *113*, 631–642.

Nagashima, H., Giannakis, C., Ashman, R.J., and Nottle, M.B. (2004). Sex differentiation and germ cell production in chimeric pigs produced by inner cell mass injection into blastocysts. Biol. Reprod. *70*, 702–707.

Nowotschin, S., and Hadjantonakis, A.K. (2020). Guts and gastrulation: emergence and convergence of endoderm in the mouse embryo. Curr. Top Dev. Biol. *136*, 429–454.

Nowotschin, S., Hadjantonakis, A.K., and Campbell, K. (2019a). The endoderm: a divergent cell lineage with many commonalities. Development *146*, dev150920.

Nowotschin, S., Setty, M., Kuo, Y.Y., Liu, V., Garg, V., Sharma, R., Simon, C.S., Saiz, N., Gardner, R., Boutet, S.C., et al. (2019b). The emergent landscape of the mouse gut endoderm at single-cell resolution. Nature *569*, 361–367.

Park, K.E., Park, C.H., Powell, A., Martin, J., Donovan, D.M., and Telugu, B.P. (2016). Targeted gene knockin in porcine somatic cells using CRISPR/Cas ribonucleoproteins. Int. J. Mol. Sci. *17*, 810.

Plusa, B., Piliszek, A., Frankenberg, S., Artus, J., and Hadjantonakis, A.K. (2008). Distinct sequential cell behaviours direct primitive endoderm formation in the mouse blastocyst. Development *135*, 3081–3091.

Ramos-Ibeas, P., Sang, F., Zhu, Q., Tang, W.W.C., Withey, S., Klisch, D., Wood, L., Loose, M., Surani, M.A., and Alberio, R. (2019). Pluripotency and X chromosome dynamics revealed in pig pre-gastrulating embryos by single cell analysis. Nat. Commun. *10*, 500.

Rashid, T., Kobayashi, T., and Nakauchi, H. (2014). Revisiting the flight of Icarus: making human organs from PSCs with large animal chimeras. Cell Stem Cell *15*, 406–409.

Rossant, J. (2008). Stem cells and early lineage development. Cell *132*, 527–531.

Rugg-Gunn, P.J., Cox, B.J., Ralston, A., and Rossant, J. (2010). Distinct histone modifications in stem cell lines and tissue lineages from the early mouse embryo. Proc. Natl. Acad. Sci. U. S. A. *107*, 10783–10790.

Seguin, C.A., Draper, J.S., Nagy, A., and Rossant, J. (2008). Establishment of endoderm progenitors by SOX transcription factor expression in human embryonic stem cells. Cell Stem Cell *3*, 182–195.

Sheets, T.P., Park, K.E., Park, C.H., Swift, S.M., Powell, A., Donovan, D.M., and Telugu, B.P. (2018). Targeted mutation of NGN3 gene disrupts pancreatic endocrine cell development in pigs. Sci. Rep. *8*, 3582.

Shen, Q.Y., Yu, S., Zhang, Y., Zhou, Z., Zhu, Z.S., Pan, Q., Lv, S., Niu, H.M., Li, N., Peng, S., et al. (2019). Characterization of porcine extraembryonic endoderm cells. Cell Prolif *52*, e12591.

Talbot, N.C., Blomberg, L.A., Mahmood, A., Caperna, T.J., and Garrett, W.M. (2007). Isolation and characterization of porcine visceral endoderm cell lines derived from in vivo 11-day blastocysts. In Vitro Cell. Dev. Biol. Anim. *43*, 72–86.

Telugu, B.P., Ezashi, T., and Roberts, R.M. (2010). The promise of stem cell research in pigs and other ungulate species. Stem Cell Rev. Rep. *6*, 31–41.

Viotti, M., Nowotschin, S., and Hadjantonakis, A.K. (2014). SOX17 links gut endoderm morphogenesis and germ layer segregation. Nat. Cell Biol. *16*, 1146–1156.

Wamaitha, S.E., del Valle, I., Cho, L.T., Wei, Y., Fogarty, N.M., Blakeley, P., Sherwood, R.I., Ji, H., and Niakan, K.K. (2015). Gata6 potently initiates reprograming of pluripotent and differentiated cells to extraembryonic endoderm stem cells. Genes Dev. *29*, 1239–1255.

West, F.D., Terlouw, S.L., Kwon, D.J., Mumaw, J.L., Dhara, S.K., Hasneen, K., Dobrinsky, J.R., and Stice, S.L. (2010). Porcine induced pluripotent stem cells produce chimeric offspring. Stem Cells Dev. *19*, 1211–1220.

Wolf, X.A., Serup, P., and Hyttel, P. (2011). Three-dimensional localisation of NANOG, OCT4, and E-CADHERIN in porcine pre- and peri-implantation embryos. Dev. Dyn. *240*, 204–210.

Wu, J., Platero-Luengo, A., Sakurai, M., Sugawara, A., Gil, M.A., Yamauchi, T., Suzuki, K., Bogliotti, Y.S., Cuello, C., Morales Valencia, M., et al. (2017). Interspecies chimerism with mammalian pluripotent stem cells. Cell *168*, 473–486.e5.

Zhao, Y., Zhao, T., Guan, J., Zhang, X., Fu, Y., Ye, J., Zhu, J., Meng, G., Ge, J., Yang, S., et al. (2015). A XEN-like state bridges somatic cells to pluripotency during chemical reprogramming. Cell *163*, 1678–1691.